International Journal for Housing Science and Its Applications
Publish August 10, 2025. Volume 46, Issue 4 Pages 3758-3773

https://doi.org/10.70517/ijhsa464499a

Study on vibration characteristics of Rigid-Frame Bridge and optimization of its damping design based on modal analysis

Mingjing Li[1], Fengwu Yu[2], Jun Tang[2,*] and Chuanyang Yang[2]
[1] Guangxi Pinglu Canal Construction Co., Ltd., Nanning, Guangxi, 530023, China
[2] CCCC First Highway Engineering Group Co., Ltd., Beijing, 100000, China
Corresponding authors: (e-mail: lunwenei333@163.com).

Abstract Continuous Rigid-Frame Bridge is a girder bridge with main girder and abutment rigidly connected to form a rigid frame, which has the advantages of good spanning ability, good overall structural performance, strong seismic capacity, etc., and can well meet the demand of transportation construction. This paper combines the theory of finite element method, finite element software ANSYS and modal analysis theory to establish the finite element model of Rigid-Frame Bridge. And the self-oscillation frequency and vibration characteristics of the model are analyzed as a way to understand the vibration characteristics of Rigid-Frame Bridge. On the basis of the finite element model of Rigid-Frame Bridge, the response characteristics of Rigid-Frame Bridge under the action of seismic waves are analyzed through the action of natural seismic waves at different angles to provide data support for the optimization of its vibration damping design. The first-order transverse self-oscillating frequency of the whole bridge obtained by the simulation of ANSYS software is 0.581Hz, and Rigid-Frame Bridge is mainly symmetrically curved with the middle span and side spans from the fifth order, which is in line with the principle of symmetrical construction of Rigid-Frame Bridges. The maximum value of transverse displacement under transverse seismic wave can reach 92.73mm, and the bridge overturning is more serious, while the effect of transverse seismic wave is smaller. Combined with the vibration characteristics and seismic response characteristics of Rigid-Frame Bridge, the optimization scheme of seismic design is proposed from the two dimensions of main girder and abutment, aiming to improve the service life and safety of Rigid-Frame Bridge.

Index Terms Rigid-Frame Bridge, finite element, vibration characteristics, transverse displacement, seismic damping design

I. Introduction

Economic development and social progress have made earthquakes more and more harmful to human beings and society, and continuous steel bridges, as transportation lifelines and hubs, will bring great hazards when earthquakes occur, affecting the relief work, and at the same time will also bring secondary disasters, resulting in great economic losses, and even leading to casualties [1]-[3]. In recent decades, a number of large-scale earthquakes have occurred around the world, bringing huge economic losses and indelible shadows for various countries, and at the same time highlighting the importance of energy dissipation and vibration damping seismic design for continuous steel bridges [4]-[6]. Generally speaking, continuous steel bridges play the role of seismic mainly rely on the high strength of the components, but this method can not avoid component damage and structural forced vibration, so it can not essentially improve the continuous steel bridge structure of energy dissipation and vibration damping anti-seismic performance, and this traditional method will also increase the cost of bridge construction [7]-[9]. Currently, continuous steel bridge structures are developing in the direction of lightweight and high strength, and in order to meet the needs of continuous steel bridge structures in terms of economy, safety, and the coordinated development of bridge functions, it is necessary to study new energy dissipation and vibration damping anti-seismic technology [10]-[12].

On the other hand, bridge structures are important hubs of the transportation system, and all the earthquakes at home and abroad have shown that damaged and collapsed bridge structures cause huge economic losses, and seriously hinder disaster relief actions and affect post-disaster recovery [13], [14]. Seismic vulnerability analysis is an effective means to evaluate the seismic performance of bridge structures. Therefore, seismic vulnerability analysis of bridge structures can be used to predict the pre-earthquake disaster of bridge structures, and according to the different vulnerability degree, the seismic capacity of bridge structures can be targeted to improve the seismic capacity of bridge structures [15]-[18].

This paper combines the finite element method and modal analysis to propose a method to analyze the vibration characteristics of Rigid-Frame Bridges, and based on the vibration characteristics of the ground vibration simulation analysis, and then put forward a specific optimization path for the vibration damping design of Rigid-Frame Bridges.

Continuous Rigid-Frame Bridge has the advantages of large overall stiffness, reasonable structural system force, no need of giant bearing for pier and beam consolidation, and convenient construction, etc. By analyzing its vibration characteristics, a new optimization path is provided for the vibration damping design of Rigid-Frame Bridge. On the basis of combing the relevant theories of finite element method and ANSYS software, the article establishes a finite element simulation model of Rigid-Frame Bridge by modal analysis of finite element method, taking a large-span Rigid-Frame Bridge in G province as the research object. The extraction of self-oscillation frequency and vibration mode characteristics is carried out for this model, and the seismic response characteristics of Rigid-Frame Bridge are analyzed by simulating natural seismic waves. Based on the analysis results, a specific plan for optimizing the seismic design of Rigid-Frame Bridge is proposed in terms of main girders and piers.

II. Theoretical computational basis of the finite element method

As the hub project of transportation lifeline, the seismic performance of bridges in strong earthquakes directly affects the rescue efficiency and economic loss after the earthquake. In order to improve the seismic capacity of bridges in strong earthquakes, it is necessary to reasonably evaluate the seismic performance of existing bridges, which can not only give effective seismic reinforcement measures, but also provide a basis for the seismic design of bridges. This chapter mainly introduces the finite element theory applied to the vibration characteristic analysis of Rigid-Frame Bridges and ground vibration simulation as well as the related knowledge of ANSYS software, which provides theoretical support for the simulation verification later.

II. A.Finite Element Method and ANSYS Software

II. A. 1) Finite element method theory

The finite element method is actually a method with the concept of discretization, which is the discretization of a whole structure on a mechanical model into a finite number of units. These units are all of a certain size and connected by a finite number of nodes, and the forces applied to each unit are used to equate the forces applied to the whole structure, thus transforming a continuous problem with no degrees of freedom into a discrete finite-degree-of-freedom problem. Each discretized unit is approximated by a simple function that can be chosen to represent the displacement distribution law of the unit, and thus the relationship between force and displacement between the unit nodes, in accordance with the energy principle in elastic mechanics [19]. Finally, by associating the relational equations of each unit, the characteristics of the finite discrete nodes on the object can be solved. The basic equations of elastic mechanics include geometric equations, equilibrium differential equations, deformation coordination equations and physical equations as follows:

(1) Geometric equations

$$[\varepsilon]=\begin{Bmatrix}\dfrac{\partial U}{\partial X}\\ \dfrac{\partial V}{\partial Y}\\ \dfrac{\partial W}{\partial Z}\\ \dfrac{\partial U}{\partial Y}+\dfrac{\partial V}{\partial X}\\ \dfrac{\partial V}{\partial Z}+\dfrac{\partial W}{\partial Y}\\ \dfrac{\partial W}{\partial X}+\dfrac{\partial U}{\partial Z}\end{Bmatrix}=\begin{bmatrix}\dfrac{\partial U}{\partial X} & \dfrac{\partial V}{\partial Y} & \dfrac{\partial W}{\partial Z} & \dfrac{\partial U}{\partial Y}+\dfrac{\partial V}{\partial X} & \dfrac{\partial V}{\partial Z}+\dfrac{\partial W}{\partial Y} & \dfrac{\partial W}{\partial X}+\dfrac{\partial U}{\partial Z}\end{bmatrix}^{T} \tag{1}$$

where ε is the strain vector, X, Y, Z are the lengths in the three coordinate directions, U, V, W are the displacements of a point along the three coordinate directions.

When the strain component $\varepsilon_X=\varepsilon_Y=\varepsilon_Z=\gamma_{XY}=\gamma_{YZ}=\gamma_{ZX}=0$, the integration of the above equation, get:

$$\begin{cases} U = U_0 + \omega_Y Z - \omega_Z Y \\ V = V_0 + \omega_Z X - \omega_X Z \\ W = W_0 + \omega_X Y - \omega_Y X \end{cases} \tag{2}$$

where U_0, V_0, W_0, ω_x, ω_Y, ω_z are integration constants.

(2) Equilibrium differential equation

$$\begin{cases} \frac{\partial \sigma_X}{\partial X} + \frac{\partial \tau_{xX}}{\partial Y} + \frac{\partial \tau_{zX}}{\partial Z} + Q_{rX} = 0 \\ \frac{\partial \tau_{XY}}{\partial X} + \frac{\partial \sigma_Y}{\partial Y} + \frac{\partial \tau_{zY}}{\partial Z} + Q_{rY} = 0 \\ \frac{\partial \tau_{XZ}}{\partial X} + \frac{\partial \tau_{rZ}}{\partial Y} + \frac{\partial \sigma_Z}{\partial Z} + Q_{rz} = 0 \end{cases} \tag{3}$$

where Q_{VX}, Q_{VT}, Q_{VZ} for the unit volume of the force in the X, Y, Z three directions of the component, σ for a direction of the positive stress, τ for a direction of the former stress, τ for a direction of the shear stress.

(3) Deformation coordination equation

The deformation coordination equation describes the continuity of an elastic object under the action of external load, which is derived from the geometric equation. Namely:

$$\begin{cases} \frac{\partial^2 \varepsilon_X}{\partial Y^2} + \frac{\partial^2 \varepsilon_Y}{\partial X^2} = \frac{\partial^2 \gamma_{xz}}{\partial X \partial Y} \\ \frac{\partial^2 \varepsilon_Y}{\partial Z^2} + \frac{\partial^2 \varepsilon_z}{\partial Y^2} = \frac{\partial^2 \gamma_{YZ}}{\partial Y \partial Z} \\ \frac{\partial^2 \varepsilon_Z}{\partial X^2} + \frac{\partial^2 \varepsilon_X}{\partial Z^2} = \frac{\partial^2 \gamma_{zr}}{\partial Z \partial X} \end{cases} \tag{4}$$

where γ is the shear strain in a given direction.

(4) Physical equations

For an elastic object, if it satisfies isotropy, the linear relationship between stress and strain satisfies the generalized Hooke's law, i.e.:

$$\begin{cases} \varepsilon_X = \frac{\sigma_X}{E} - \mu \frac{\sigma_Y}{E} - \mu \frac{\sigma_Z}{E} \\ \varepsilon_Y = \frac{\sigma_Y}{E} - \mu \frac{\sigma_Z}{E} - \mu \frac{\sigma_X}{E} \\ \varepsilon_Z = \frac{\sigma_Z}{E} - \mu \frac{\sigma_X}{E} - \mu \frac{\sigma_Z}{E} \\ \gamma_{XY} = \frac{\tau_{XY}}{G} \gamma_{YZ} = \frac{\tau_{YZ}}{G} \gamma_{ZX} = \frac{\tau_{ZX}}{G} \end{cases} \tag{5}$$

where, E is the modulus of elasticity, μ is Poisson's ratio, G is the shear elastic modulus, and $G = \frac{E}{2(1+\mu)}$.

The calculation steps of the finite element method mainly include the discretization of the continuous medium, the analysis of the mechanical properties of the unit and the overall analysis. The main task of the discretization of the continuous medium is to determine the appropriate type of unit, divide the continuous medium into a finite number of units, impose constraints on the structure, and convert the loads acting on the structure into nodal loads. Unit mechanical characterization is to analyze the mechanical properties of the divided unit, the key is to get the relationship between the unit node force and its displacement. The overall analysis is to connect the units through the nodes into the original continuum analysis process, that is, the balance equations of each unit grouped into the overall equilibrium equations.

II. A. 2) Finite element software ANSYS

ANSYS is a multi-purpose finite element analysis software, which has a variety of different analysis modules, such as structural, fluid, electric field, magnetic field, acoustic field analysis, and has a matching interface and data sharing with other computer design software. The specific flow of the ANSYS finite element analysis is shown in Fig. 1, which mainly consists of three phases: pre-processing, loading and solving, and post-processing [20].

(1) Pre-processing stage. When performing finite element analysis calculations, the analysis problem needs to be modeled (materialized) and discretized. Modeling refers to the transformation of the actual problem of the analysis into a two-dimensional model, three-dimensional solid processing, discretization processing, that is, the analytical model mesh division processing. At the same time, in order to improve the efficiency of analysis and calculation, in the pre-processing stage also needs to be given to analyze the material properties of the geometric model.

(2) Load solving stage. Need to be based on the actual situation in the software to set constraints on the solution model, the setting of boundary conditions will affect the accuracy of the solution calculation. In addition, it is also necessary to set the solution options in the software, such as the application of load sub-steps, time sub-steps, the selection of the type of solution, and so on.

(3) Post-processing stage. According to the required type of solving data in the auxiliary calculation software solving options to add the choice, while the software analysis of the calculated results should be compared with the actual theoretical values. Thus, check whether the data processed in the previous stage and the added boundary conditions are reasonable and feasible.

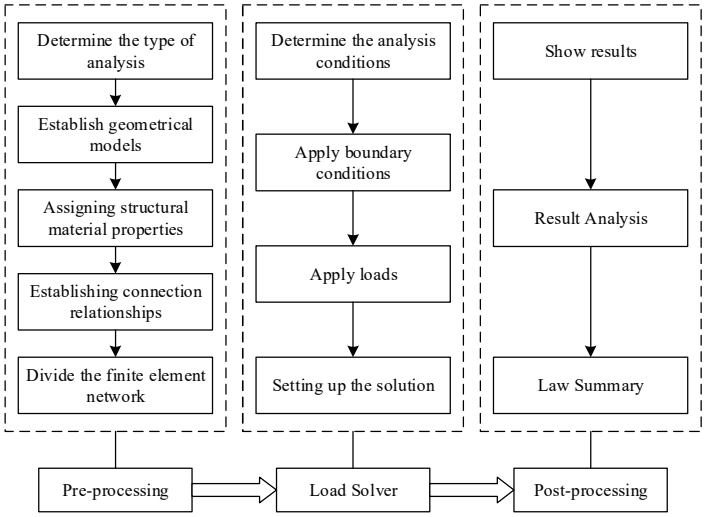

Figure 1: ANSYS finite element analysis specific process

II. B.Application of Finite Element Method in the Analysis of Reinforced Concrete Structures

II. B. 1) Modeling of the intrinsic relationship of concrete materials

Concrete is a composite material with a very complex internal composition and a heterogeneous microstructure when viewed microscopically and macroscopically respectively. The macroscopic can be regarded as a two-phase material with aggregates dispersed in the cement paste. Different perspectives of scholars and different application scenarios make the ontological relationships of concrete much different. Nonlinear elasticity theory and elastoplasticity theory have their scope of application and are usually applied in nonlinear finite element analysis of concrete materials.

In ANSYS modeling and analysis, the isotropic nonlinear elasticity principal relationship can be used for concrete material principal relationship [21]. Regarding the damage criterion of concrete, it is important to understand the damage mechanism of concrete to establish this criterion in the nonlinear analysis of concrete. When concrete destroys, its state of stress and strain needs to satisfy certain conditions, which is what the damage criterion describes. In this paper, we mainly choose the W-W five-parameter criterion, which is default in ANSYS software. Namely:

$$\frac{\tau_{mt}}{f_c} = a_0 + a_1\frac{\sigma_m}{f_c} + a_2\left(\frac{\sigma_m}{f_c}\right)^2 \quad \theta = 0^0 \tag{6}$$

$$\frac{\tau_{mc}}{f_c} = b_0 + b_1\frac{\sigma_m}{f_c} + b_2\left(\frac{\sigma_m}{f_c}\right)^2 \quad \theta = 60^0 \tag{7}$$

where the hydrostatic compressive stress is represented by σ_m, the average shear stress is represented by τ_m, the uniaxial compressive strength of concrete is represented by f_c, and θ is the Haigh-Westergaard stress space

coordinates, where the parameters, a_0, a_1, a_2, b_0, b_1, and b_2, five of which are independent, can be determined by the strength of the material test.

II. B. 2) Modeling the relationship between reinforcing steel and concrete

For the modeling of the relationship between reinforcement and concrete, which mainly exists differently in different phases, this paper only considers the modeling of the relationship between reinforcement and concrete in the elastic phase of uncracked Rigid-Frame Bridges. This stage occurs before cracks appear, and the deformations occurring in reinforcement and concrete are due to the motion of atoms, which are macroscopically in the elastic stage.

The modulus of elasticity of the stiffened bridge beams is derived from the bending beam theory, i.e., the combined force in the beam cross-section is zero and the combined moment formed by the combined force is equal to the bending moment of the cross-section. The modulus of elasticity at this stage is derived by analyzing the forces and moments in the cross-section based on the measured tensile and compressive strains in the following procedure. According to the theory of inelastic bending of Rigid-Frame Bridge girders, then:

$$\begin{cases} \int_{\varepsilon^c}^{z^t} \sigma d\varepsilon = 0 \\ M = \dfrac{bh^2}{\varepsilon_t^2} \int_{\varepsilon^c}^{z^t} \sigma \varepsilon d\varepsilon \end{cases} \tag{8}$$

Based on the above equation, with known strain and bending moment:

$$\begin{cases} \sigma_1^t = \dfrac{3M_1\varepsilon_{t1}}{bh^2\varepsilon_1^t} \\ \sigma_1^c = \dfrac{3M_1\varepsilon_{t1}}{bh^2\varepsilon_1^c} \end{cases} \tag{9}$$

$$\begin{cases} E_i^t\left(\varepsilon_i^t - \varepsilon_{i-1}\right)^2\left(2\varepsilon_{ti} + \varepsilon_{t(i-1)}\right) = \dfrac{6\left(M_i{\varepsilon_{ti}}^2 - M_{i-1}{\varepsilon_{t(i-1)}}^2\right)}{bh^2} \\ +{\sigma_{i-1}}^c\left(\varepsilon_i^c - {\varepsilon_{i-1}}^c\right)^2 \\ -{\sigma_{i-1}}^t\left(\varepsilon_i^t - {\varepsilon_{i-1}}^t\right)\left[3\left(\varepsilon_{it} + \varepsilon_{t(i-1)}\right) + \left(\varepsilon_i^c - {\varepsilon_{i-1}}^c\right)\right] \\ E_i^c\left(\varepsilon_i^c - \varepsilon_{i-1}^c\right)^2\left(2\varepsilon_{ti} + \varepsilon_{t(i-1)}\right) = \dfrac{6\left(M_i{\varepsilon_{ti}}^2 - M_{i-1}{\varepsilon_{t(i-1)}}^2\right)}{bh^2} \\ +{\sigma_{i-1}}^t\left(\varepsilon_i^t - {\varepsilon_{i-1}}^t\right)^2 \\ -{\sigma_{i-1}}^c\left(\varepsilon_i^c - \varepsilon_{i-1}^c\right)\left[3\left(\varepsilon_{ti} + \varepsilon_{t(i-1)}\right) + \left(\varepsilon_i^t - {\varepsilon_{i-1}}^t\right)\right] \end{cases} \tag{10}$$

$$\begin{cases} \sigma_i^t = {\sigma_{i-1}}^t + E_i^t\left(\varepsilon_i^t - {\varepsilon_{i-1}}^t\right) \\ \sigma_i^c = {\sigma_{i-1}}^c + E_i^c\left(\varepsilon_i^c - {\varepsilon_{i-1}}^c\right) \end{cases} \tag{11}$$

where bending moments $M_i = P_i L/4$ and P_i are measured loads, ε_i^t and ε_i^c are measured tensile and compressive strains, E_i^t and E_i^c are the required tensile and compressive modulus of elasticity at each stage, and σ_i^t and σ_i^c are the tensile and compressive stresses derived from the modulus of elasticity $(i = 1, 2, 3, \cdots)$. Measured tensile and compressive strains result in the position of the neutral axis floating up and down and not being fixed, which is characteristic of a material with microcracks.

III. Modal analysis of continuous rigid frame bridges

With the growth of service life, under the influence of various objective factors, both internal and external, the performance of reinforced concrete structures will inevitably decline, leading to changes in the overall structural stiffness and bearing capacity, which may have a non-negligible impact on the seismic resistance of the structure. In order to deeply analyze the relevant parameters affecting the seismic performance of Rigid-Frame Bridges, and then provide a reference for the optimized design of Rigid-Frame Bridges for vibration reduction, this chapter mainly focuses on the vibration characteristics of Rigid-Frame Bridges using modal analysis to conduct quantitative research.

III. A. Theoretical Foundations of Modal Analysis

III. A. 1) Modal Analysis Theory

Modal analysis is a technique used to determine the vibration characteristics of a structure, including the infinite order intrinsic frequency and its corresponding vibration modes of each order, as well as the mode participation coefficients, i.e., the degree of participation of the vibration modes in a given direction. These parameters are important factors that must be considered when designing a structure to withstand dynamic loading, and are also the basis for performing various other types of dynamic analysis [22].

The basic equation for dynamic analysis is:

$$[M]\{\ddot{u}\}+[C]\{\dot{u}\}+[K]\{u\}=\{F(t)\} \tag{12}$$

Where, $[M]$ is the structural mass matrix, $[C]$ is the structural damping matrix and $[K]$ is the structural stiffness matrix. $\{\ddot{u}\}$ is the acceleration vector of the node, $\{\dot{u}\}$ is the velocity vector of the node, $\{u\}$ is the displacement vector of the node, and $\{F(t)\}$ is the time-dependent load function.

In the modal analysis, the dynamic equations when free vibration and neglecting the structural damping are:

$$[M]\{\ddot{u}\}+[K]\{u\}=\{0\} \tag{13}$$

When harmonic vibration occurs, then the equation is:

$$\left([K]-\omega_i^2[M]\right)\{\phi_i\}=\{0\} \tag{14}$$

Therefore, when a member is subjected to modal analysis, its intrinsic frequency ω_i and mode ϕ_i can be obtained by solving the modal equations.

Modal analysis is a typically linear analysis technique that ignores any nonlinear features. By performing modal analysis on a model, it can be designed to avoid resonance or to vibrate at a specific frequency as required for the job. In addition, it is possible to understand the vibration of the component under different dynamic loads and provide guidance for the control parameters in other dynamic analyses.

Low-order modes are mesh-independent, so relatively coarse meshes can be used to save computational resources. Special attention should be paid to.

(1) If there are only partial constraints or no constraints, a rigid-body mode will be obtained with an intrinsic frequency in the neighborhood of 0 Hz.

(2) Since the boundary conditions affect the intrinsic frequency and vibration pattern of the member, the constraints need to be carefully considered in the modal analysis, and this feature can also be used to check whether the model is fully constrained.

(3) Modal analysis is linear and automatically ignores any nonlinear features. Since compression constraints are nonlinear, they may exhibit properties similar to frictionless constraints.

III. A. 2) Finite element method for modal analysis

The vibration differential equation of a Rigid-Frame Bridge as a multi-degree-of-freedom vibration system with multiple vibration sources superimposed is:

$$M\ddot{x}(t)+C\dot{x}(t)+Kx(t)=f(t) \tag{15}$$

where M is the total mass matrix of the system, C is the total damping matrix of the system, K represents the total stiffness matrix of the system, $x(t)$ is the displacement response vector of the nodes, $\dot{x}(t)$ is the velocity response matrix, $\ddot{x}(t)$ is the acceleration response matrix, $f(t)$ represents the excitation force vector of the structure.

To solve the dynamics of Rigid-Frame Bridge structure, modal analysis of the main features of Rigid-Frame Bridge intrinsic frequency and the corresponding vibration mode, often ignoring the smaller damping, the above equation is transformed into:

$$M\ddot{x}(t)+Kx(t)=0 \tag{16}$$

Its simple harmonic motion converts to:

$$X=X_0\cos(\omega t+\varphi) \tag{17}$$

where X_0 is the vibration mode of each node, ω is the frequency corresponding to the vibration mode, and φ is the phase angle.

Substituting (17) into (16) yields:

$$\omega_1^2<\omega_2^2<\omega_3^2<\cdots<\omega_n^2 \tag{18}$$

Based on the fact that their vibrational modes are not all equal to zero, from Eq. (18):

$$K-\omega^2 m=0 \tag{19}$$

where K is the n nd order stiffness equation, M is the n th order mass equation, and n is the number of node degrees of freedom.

Eq. (19) is a n th order equation with n solutions, whose solution is the natural frequency of the stiffened bridge.

The vibration displacement is expressed as:

$$\begin{aligned} X=&\{X_0\}_1\cos(\omega_1 t+\phi_1)+\{X_0\}_2\\ &\cos(\omega_2 t+\phi_2)+\cdots+\{X_0\}_n\cos(\omega_n t+\phi_n)\end{aligned} \tag{20}$$

where $\{X_0\}_i$ is the vibration mode corresponding to each self-oscillation frequency.

The finite element analysis software has many modal extraction methods, based on the differences of the structure in the specific analysis examples, and the specific requirements of the structural solution accuracy and other parameters of the modal analysis, it is necessary to choose the optimal modal extraction method. Block Lanczos method and subspace iteration method are commonly used in engineering applications. In order to effectively extract the modes and combine with the model characteristics of Rigid-Frame Bridge structure, Block Lanczos method is chosen in this paper.

III. B. Finite element modeling of steel bridge

III. B. 1) Summary of works

In order to deeply analyze the vibration characteristics of rigid-frame bridges, this paper takes a large-span rigid-frame bridge in Province G as the research object, and its bridge arrangement is shown in Fig. 2. The superstructure adopts three-way prestressed single box and single chamber variable cross-section, and the span composition is 100m+160m+100m. The width of the box girder top plate is 12.5m, and the width of the bottom plate is 7.2m, and the girder height varies from 3.6m in the middle of the span to the root of the box girder of 11.6m with a 1.6 parabolic change, and the thickness of the bottom plate of the box girder varies from 1.4m in the root cross-section to the middle of the span and the pivot cross-section of the side spans of 0.34m with a 1.8 parabolic gradient. The bridge is divided into 25 (10*3m and 15*5m) hanging basket cantilever casting sections, the side and middle span merging section are 2.5m, the side span casting section is 4m long. 5# pier of the bridge substructure adopts hollow thin-walled box section with pier height of 98m, and 5# pier adopts double-limb thin-walled pier with pier height of 45m.

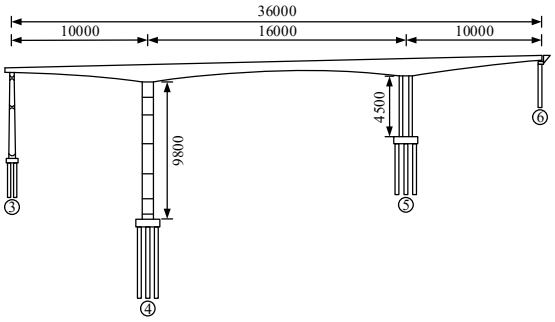

Figure 2: A schematic diagram of the bridge

III. B. 2) Finite element modeling

The paper adopts ANSYS finite element analysis software to establish the three-dimensional solid model of the case large-span continuous Rigid-Frame Bridge, which mainly includes the establishment of abutments and main span members, applying loads to different nodes of the bridge and setting constraints. In modeling the main girders and abutments, the bridge suspension construction section is refined by simulation through the beam cell method. When modeling and parameterizing the bridge, the effect of the quality of the reinforcement can be ignored since the loads carried by the steel bars only account for a relatively small portion of the overall loads. The concrete density was 26 kN/m3 and the stress limit of the longitudinal reinforcement was 1500 MPa in tension. Considering the load bearing situation during construction, the hanging basket with pedestrian load is 850kN. For Phase II constant loads such as infrastructure, mortar bedding and concrete footings, the load per unit length is estimated to be 125kN/m. During the bridge construction process, it is assumed that the girders undergo a uniform warming and cooling process with a magnitude of 27°C in order to assess the impact of temperature changes on the bridge.

In accordance with the requirements of the design specification, the quantitative assessment of wind loads should be calculated and imposed based on the following equation when performing bridge simulation analysis, i.e:

$$W=P_1P_2P_3W_0 \tag{21}$$

Where W_0 is the basic wind load standard intensity value (Pa), P_1 is the morphology parameter of wind loaded bridge members, P_2 is the change parameter of wind load intensity along the bridge height, and P_3 is the parameter of site condition of the bridge site.

From Eq. It can be seen that the wind loads in both longitudinal and transverse bridge directions are mainly considered in assessing the wind loads on the bridge. The minimum and maximum values of wind load in the transverse direction are 1146.3 Pa and 1283.7 Pa, respectively. The minimum and maximum values of wind load in the longitudinal direction are 985.4Pa and 1076.5Pa, respectively, so that the wind load in the transverse direction and longitudinal direction take the range of 1146.3~1283.7Pa and 985.4~1076.5Pa, respectively. The bottom of the piers is set as fixed connection, while the corresponding nodes of the main pier and the zero block are rigidly connected. Based on the above process of modeling and parameter setting, the finite element model of the large-span continuous Rigid-Frame Bridge is shown in Fig. 3.

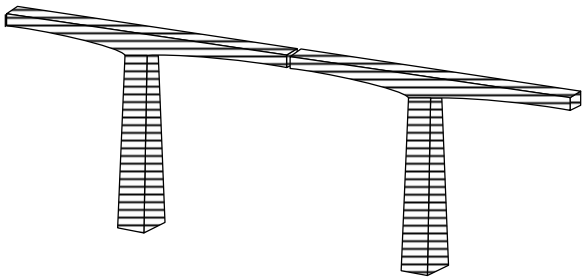

Figure 3: The finite element model of the large cross continuous rigid frame

III. C. Modal analysis calculation results

III. C. 1) Frequency comparison analysis

In order to analyze the vibration characteristics of the selected research object, in this paper, in addition to using ANSYS finite element software for Rigid-Frame Bridge modeling, the models established by Midias Civil and Simpack finite element software are also used for comparative analysis. The self-oscillation frequency distributions of the finite element models established by different software under no external load are shown in Table 1.

Compared with the model established by Simpack's finite element software, it can be seen that the difference between the first ten frequencies of the finite element model established by Midias Civil and Simpack is no more than 3.64% (the difference between the second-order frequencies is 3.64%), and the difference between the first ten frequencies of the finite element model established by ANSYS and Simpack is no more than 0.46% (the difference between the sixth-order frequencies is 0.46%), which illustrates Midias The accuracy of the finite element models created by the Civil and Simpack software is slightly lower than that of the finite element models created by the ANSYS software. To a certain extent, the feasibility of using ANSYS software to analyze the vibration characteristics of long-span Rigid-Frame Bridges is verified.

In addition, from the results of the self-resonance frequency of the large-span steel bridge, the first-order lateral self-resonance frequency of the whole bridge from ANSYS, Midias Civil, and Simpack are 0.581Hz, 0.572Hz, and 0.583Hz, respectively, and the corresponding first-order transverse self-resonance periods are 1.694s, 1.763s, and 1.697s.The specification does not specify the limits of the overall lateral self-resonance frequency of the long-span continuous girder and continuous The overall transverse self-oscillation frequency limit for large-span continuous girder and continuous rigid frame bridge is not specified in the specification. Referring to the “Railway Bridge Inspection Code”, it is stipulated that the measured minimum transverse self-oscillation frequency of simply supported bridges is usually $[f] \geqslant 90/L$ when passenger and freight or wagon trains are in normal operation, where L is the length of the main span of the continuous rigid structure. That is, the transverse self-oscillation frequency of the whole bridge is not less than 0.562 Hz. Therefore, according to the above requirements, the continuous rigid structure of the bridge with a main span of 160 m meets the above requirements for the transverse first self-oscillation frequency.

III. C. 2) Modal analysis of vibration patterns

ANSYS provides seven methods for extracting modes, the first four being the chunked Lanczos method, the Subspace method, the Power Dynamics method, and the Reduce/Householder method. In this paper, the default default chunked Lanczos method is used, which is faster and has the same accuracy as the subspace method when extracting modes of more orders. The dynamic characteristics of a bridge structure refer to the intrinsic frequency and the vibration mode of the bridge, and Fig. 4 shows the vibration mode characteristics of a large-span Rigid-Frame Bridge, in which Fig. 4(a)~(j) shows the vibration mode characteristics of the 1st to 10th orders, respectively.

According to the model in Fig. 4, the first 10 orders of self-oscillation frequency and vibration mode characteristics are shown in Table 2.

Table 1: The vibration frequency of non-external load

First order	Midias Civil (Hz)	Simpack (Hz)	Difference ratio	ANSYS (Hz)	Simpack (Hz)	Difference ratio
1	0.572	0.583	1.92%	0.581	0.583	0.34%
2	0.851	0.882	3.64%	0.879	0.882	0.34%
3	0.954	0.976	2.31%	0.976	0.976	0.00%
4	1.267	1.235	2.53%	1.232	1.235	0.24%
5	1.503	1.463	2.66%	1.463	1.463	0.00%
6	1.938	1.947	0.46%	1.938	1.947	0.46%
7	2.056	2.031	1.22%	2.026	2.031	0.25%
8	2.323	2.358	1.51%	2.357	2.358	0.04%
9	2.389	2.392	0.13%	2.389	2.392	0.13%
10	2.406	2.415	0.37%	2.403	2.415	0.50%

From the results of computational analysis and the first ten orders of vibration pattern diagram of Rigid-Frame Bridge, the following conclusions can be drawn:

(1) In the first ten orders of vibration pattern of this model, including the vibration of abutment and bridge, the vibration pattern is more different, and the vibration pattern of the first few orders of vibration pattern is dominated by vertical bending.

(2) The base frequency of this bridge is larger, indicating that the overall structural rigidity of the bridge is larger, and the vibration pattern is symmetrical vertical bending of the main girder midspan of the first order. This vibration mode is symmetrical vertical bending of the main girder midspan, instead of longitudinal drift of the main girder. This is a structural characteristic of the main girder and pier cementation. Therefore, it is greatly affected by vertical seismic response and wind stability, and at the same time, the response to vehicle vibration is also larger.

(3) The first three orders of vibration of this bridge are dominated by vertical bending, when the vertical seismic response is the largest.

(4) The torsional vibration pattern of the bridge deck appears later, indicating that the torsional stiffness of the structure is larger, and it is easier to meet the stiffness requirements.

(5) The vibration patterns appearing in the later orders are dominated by the symmetrical bending of the center span and side spans, indicating that the design of this bridge follows the principle of symmetry. The overall intrinsic frequency of this bridge is high, and the stiffness is large, which should deal with the problem of resonance caused by the similar frequency of external loads.

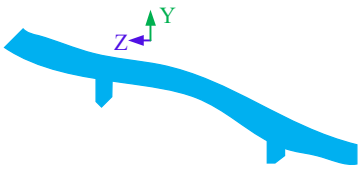

(a) First-stage

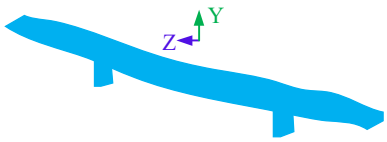

(b) Second stage

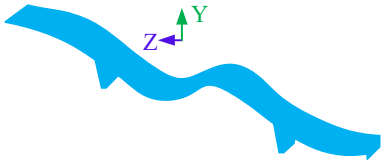

(c) Third stage

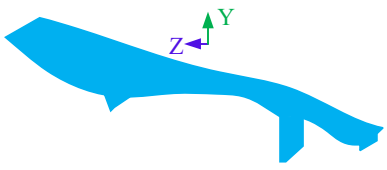

(d) Fourth stage

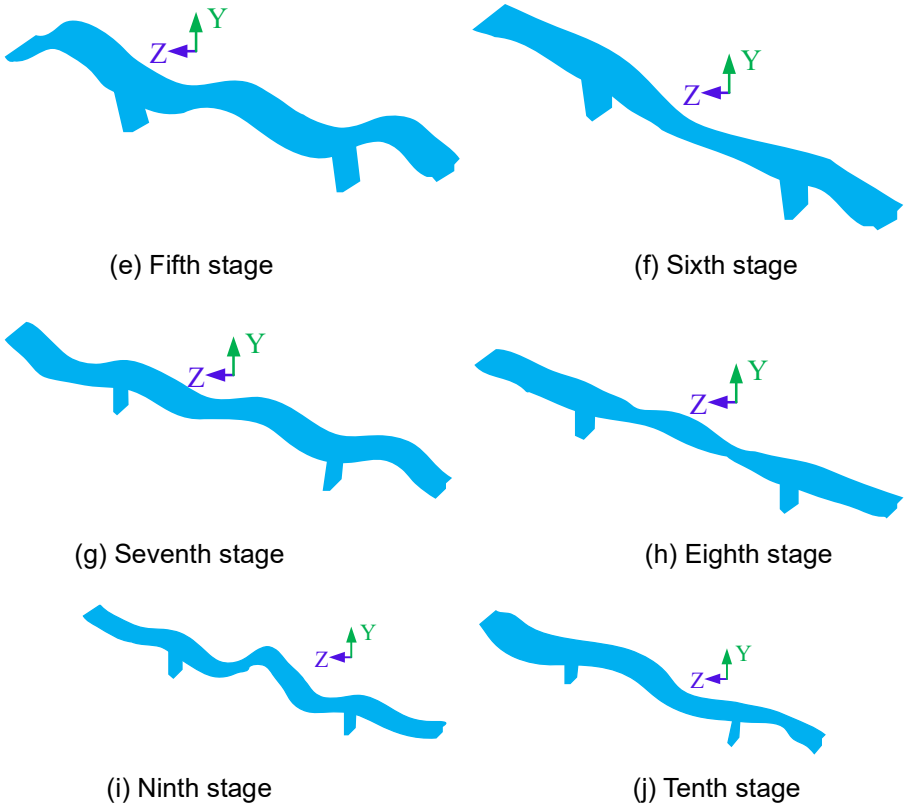

(e) Fifth stage (f) Sixth stage

(g) Seventh stage (h) Eighth stage

(i) Ninth stage (j) Tenth stage

Figure 4: The type of vibration of the large cross rigid frame

Table 2: Vibration frequency and vibration characteristics

First order	Frequency (Hz)	Vibration characteristic
1	0.581	The main beam is symmetrical vertically
2	0.879	The main beam is symmetrical vertically
3	0.976	The main beam is opposed to the vertical bend+ Cross the first order opposition
4	1.232	The cross bending and the lateral bending of the opposite
5	1.463	Cross against+ Edge span counterclaim Cross bending
6	1.938	Middle and second symmetric vertical bending+ The edge of the symmetry is curved
7	2.026	Intersymmetrical torsion+ Lateral cross-symmetric torsion
8	2.357	Middle and second opposition is opposed to vertical bending+ The side is opposed to the vertical bend
9	2.389	Middle and second symmetric vertical bending+ The edge of the symmetry is curved
10	2.403	The opposite is called torsion+ Edge span counterclaim Cross bending

IV. Optimization analysis of seismic design for Rigid-Frame Bridges

In the bridges under construction or have been constructed in western China, high pier continuous rigid-frame bridges are dominated by gravity piers, and high pier bridges with a height of more than 40m account for more than 40%. The main feature of high pier Rigid-Frame Bridge girders is that the piers account for a high proportion of the weight of the bridge, and the length to slenderness ratio is large. The western mountainous area is located between the seismic zone of Eurasia, which is a high seismic region, and the basic intensity of the earthquake is above 6 degrees, resulting in the region's large-span high-pier railroad bridges face outstanding seismic problems. How to realize the optimization of the seismic design of rigid-frame bridges has become a problem that must be considered to ensure the safety of bridges at present. In this chapter, based on the finite element model of Rigid-Frame Bridge established in the previous section, the seismic response characteristics are analyzed by simulating seismic waves to provide support for the optimized design of Rigid-Frame Bridge for seismic mitigation.

IV. A. Selection and input of ground shocks

IV. A. 1) Natural Seismic Wave Selection

In this paper, the natural seismic waves are selected through the design response spectrum of the bridge with the bridge gauge generation algorithm, and Table 3 shows the details of the seven seismic waves selected, and the loading direction is the horizontal direction of the bridge. The seismic waves with serial numbers 1~7 are amplitude-modulated to 0.45g, and the damping model adopts Rayleigh damping with a damping ratio of 4%.

Table 3: Natural seismic wave information

No.	Code	Name	Step length	Duration	Magnitude	MSE
1	RSN15	Kern Country	0.006	69.99	7.35	0.035
2	RSN38	Borrego Mtn	0.006	50.45	6.64	0.076
3	RSN42	Borrego Mtn	0.006	52.48	6.64	0.028
4	RSN53	San Fernando	0.006	70.01	6.62	0.099
5	RSN75	San Fernando	0.006	35.99	6.62	0.038
6	RSN78	San Fernando	0.006	26.27	6.62	0.104
7	RSN86	San Fernando	0.006	27.75	6.62	0.042

IV. A. 2) Ground vibration input method

According to the following two equations, the parallel fault component SP and vertical fault component SN are rotationally transformed to find the longitudinal bridge-oriented seismic wave input X_θ and the transverse bridge-oriented seismic wave input Y_θ as:

$$X_\theta = SP \cdot \cos\theta + SN \cdot \sin\theta \tag{22}$$

$$Y_\theta = SN \cdot \cos\theta - SP \cdot \sin\theta \tag{23}$$

where θ is the angle between the fault strike and the bridge axis, SP is the component originally parallel to the fault, and SN is the component originally perpendicular to the fault.

When the bridge axis is $\theta = 0°$ parallel to the fault strike, the longitudinal bridgeward input $X_0 = SP$ is taken at this time, and the SP component corresponding to PGA 0.5g, 0.6g, and 0.7g, respectively, and the same proportion adjustment is made for the SN and bridgeward ground vibration, and thereafter the PGA is not adjusted when the effect of the angle of entrapment is taken into account. Existing studies show that the PGA peak values are approximated to be in the range of 0.5g to 0.7g in the range of 5 to 10km from the fault. The angle between the fault strike and the bridge axis θ is divided by 15° spacing for 13 conditions of 0°, 15°, 30°, 45°, 60°, 75°, 90°, 105°, 120°, 135°, 150°, 165°, and 180°. To clarify, when only elastic analysis is considered and only the maximum response is concerned, only the cases from 0° to 90° can be analyzed. For elastic-plastic response analysis, due to the asymmetry of seismic waves (even more so for near-fault ground shaking), it is necessary to consider the cases from 0° to 180°.

IV. B. Seismic Response of Continuous Rigid-Frame Bridges

IV. B. 1) Maximum internal force and displacement response

In this paper, the maximum internal forces and displacements at mid-span, top of pier and bottom of pier are simulated by using transverse seismic wave input. Table 4 shows the maximum internal force and displacement response under simulated seismic wave.

According to the data in the table, the following conclusions can be drawn:

(1) For the maximum internal forces and displacements in a typical section - mid-span, the larger value of transverse shear in the mid-span section occurs in the second span, with a transverse shear value of 2.26*105N. The larger value of transverse bending moment in the mid-span section occurs in the second span, with a transverse moment value of 4.87*107N·m. The larger value of torque in the mid-span section occurs in the second span as well as the larger value of transverse bending moment, with the value of torque in the second span being 4.23*106. The larger transverse displacements in the mid-span section occur in the mid-span, with the largest transverse displacement in the mid-span section of the second span, which has a value of 1.09*10-2m.

(2) For the maximum internal force and displacement response of a typical section-pier top, the larger values of transverse shear at the pier top location occur at pier 3 and 4, with values of 2.72*106N and 8.58*106N, respectively, and the maximum transverse shear at the top of pier 4. The larger value of the transverse bending moment at the pier top location occurs at Pier 4, whose pier top transverse bending moment value is 3.51*107N·m. The larger value of torque at the location of pier top occurs at pier 6 with a value of 7.08*106N·m. The larger value of lateral displacement at the location of the top of the pier occurs at pier 3 with a value of 6.45*10-4m.

(3) For the maximum internal force and displacement response of the typical section-pier bottom, the larger values of transverse shear at the pier bottom location appear in the middle of pier 4 and pier 5 pier bottom, whose values are 1.98*107N, 1.21*107N, respectively, with the largest value of transverse shear at the pier bottom of pier 4. The larger value of torque at the bottom of the pier also appeared at the bottom of the middle pier No. 4 and No. 5, and its value was 3.79*108N·m, 1.63*108N·m. The larger value of transverse bending moment at the bottom of the pier appeared at the pier No. 5, and the value of transverse bending moment was 3.52*107N·m.

Table 4 Max internal force and displacement response

Section - Span				
Section position	Transverse shear (N)	Transverse bending moment (N·m)	Torque (N·m)	Lateral displacement (m)
First cross	$1.43*10^5$	$4.55*10^7$	$5.42*10^5$	$1.03*10^{-2}$
Second cross	$2.26*10^5$	$4.87*10^7$	$4.23*10^6$	$1.09*10^{-2}$
Third cross	$1.42*10^5$	$4.51*10^7$	$4.06*10^5$	$1.02*10^{-2}$
Section - Pier top				
Section position	Transverse shear (N)	Transverse bending moment (N·m)	Torque (N·m)	Lateral displacement (m)
Block 3	$2.72*10^6$	$7.93*10^6$	$3.05*10^6$	$6.45*10^{-4}$
Block 4	$8.58*10^6$	$3.51*10^7$	$5.23*10^6$	$1.65*10^{-3}$
Block 5	$1.39*10^6$	$4.93*10^6$	$4.87*10^6$	$4.98*10^{-3}$
Block 6	$1.35*10^6$	$2.35*10^6$	$7.08*10^6$	$5.22*10^{-3}$
Section - Bottom				
Section position	Transverse shear (N)	Torque (N·m)	Transverse bending moment (N·m)	
Block 3	$5.15*10^6$	$6.03*10^7$	$8.28*10^6$	
Block 4	$1.98*10^7$	$3.79*10^8$	$6.07*10^6$	
Block 5	$1.21*10^7$	$1.63*10^8$	$3.52*10^7$	
Block 6	$4.53*10^6$	$4.75*10^7$	$8.93*10^6$	

IV. B. 2) Characterization of seismic wave response

(1) Characteristics of seismic wave response in the downstream direction

In order to study the effect of seismic action on the bridge structure, this paper extracts the main girder displacement with position change curves in different directions under the seismic source with the angle of 0° in the downstream direction, and its specific distribution is shown in Fig. 5. The position numbering sequence is from the left girder end to the right girder end, and Fig. 5(a)~(c) indicates the displacement in the crossover direction, transverse direction and vertical direction in turn.

The results show that under the action of seismic wave in the crossover direction, the crossover displacement presents the phenomenon that the main girder span is large and the two sides are small, and the maximum and minimum values of the displacement appear in the main girder span, with the values of 0.63mm and -0.92mm, which are small. This is due to the fact that the girder end of the main girder restricts the displacement and cornering in the transverse direction, and the deformation is mainly caused by the deformation of the main girder structure itself. The transverse displacement shows periodic changes, reaching the minimum at the pier-beam consolidation and the maximum near the center of No.3 span girder, with the maximum and minimum values of 0.03mm and -0.03mm, respectively.Under the action of seismic wave in the downstream direction, the transverse direction almost does not produce deformation. Vertical displacements show a periodic symmetrical distribution, reaching a maximum near the center of the main girder span in the range of spans 4 and 5, with maximum and minimum values of 1.39 mm and -1.39 mm, respectively.Comparison of the displacements in the downstream, transverse, and vertical directions reveals that the vertical direction of the bridge is most affected by the downstream seismic wave.

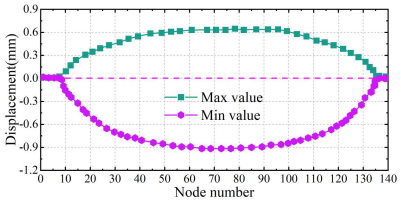

(a) Horizontal displacement

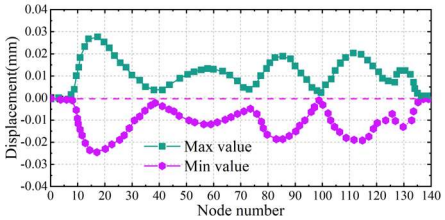

(b) Transverse displacement

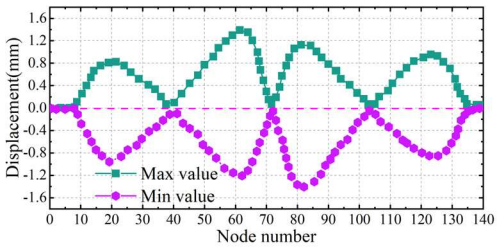

(c) Vertical displacement

Figure 5: The normal bridge is characterized by seismic wave response

(2) Characterization of seismic wave response in transverse direction

The displacement of the main girder in different directions under the seismic source with an angle of 90° in the direction of the bridge is shown in Fig. 6. The position numbering sequence is from the left beam end to the right beam end, and Fig. 6(a)~(c) shows the displacement in the downstream direction, the transverse direction and the vertical direction in turn.

The results show that, under the action of transverse seismic wave, the transverse displacement shows periodic changes, and the maximum and minimum values appear near the middle of span No. 3, with the values of 0.011mm and -0.011mm, which can be seen that the values are very small, and basically no transverse displacement is generated under the action of transverse seismic wave. The transverse displacement shows the phenomenon that the middle is big and the two sides are small, and the maximum and minimum values are 92.73mm and -72.97mm in turn. Under the action of transverse seismic wave, the bridge overturning is more serious, and the influence on the main girder span center reaches the maximum. Vertical displacement shows periodic changes, the maximum and minimum values are 0.12mm and -012mm in turn, which can be seen that the value is very small. From the comparison of the three directions, namely, along-bridge direction, transverse direction and vertical direction, it can be seen that under the transverse direction seismic wave, the impact on the bridge transverse direction is the largest.

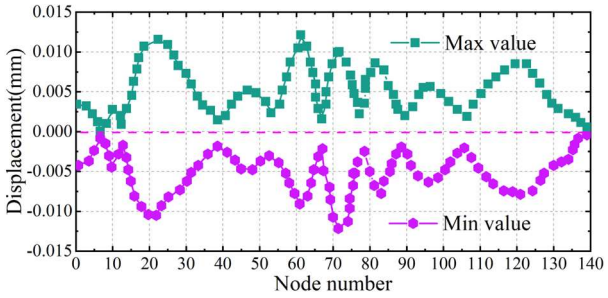

(a) Horizontal displacement

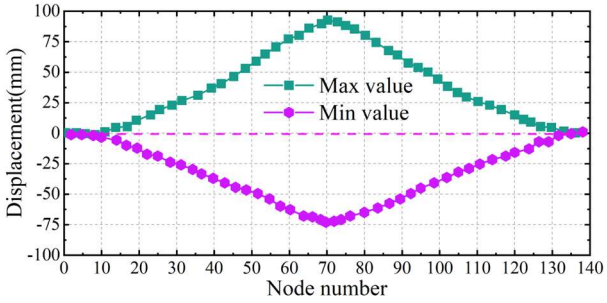

(b) Transverse displacement

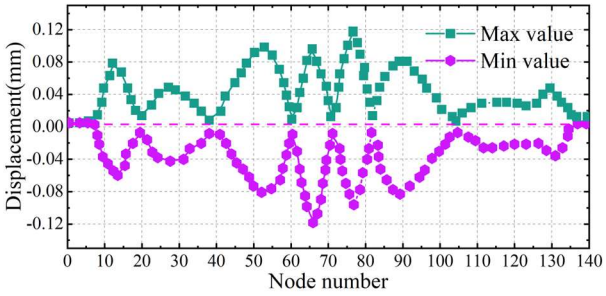

(c) Vertical displacement

Figure 6: Transverse bridge to seismic wave response characteristics

IV. C. Optimization of Seismic Damping for Continuous Rigid Frame Bridges

IV. C. 1) Main beam optimization

(1) Side-mid-span ratio. The midspan span of the main bridge is 160m, and the variation range of the ratio of side span to midspan span is 0.45~0.75, each time incremented by 0.2. Within the online elasticity range, the work done by the external force acting on the main girder is measured by the bending strain energy accumulated in the girder. Neglecting the effect of prestressing tendons, the bending moment envelope diagram of the model at the limit state of load carrying capacity was used to calculate the unit bending energy. The smaller the value of unit bending energy, the smaller the external load bending moment per linear meter for the whole bridge, which to some extent reflects the degree of influence of external load on continuous girder bridges. Therefore, for the continuous Rigid-Frame Bridge with main span diameter between 120~180m, it is recommended that the span ratio between side span and center span be controlled in the range of 0.47~0.56 to ensure that the bridge achieves better structural performance in the construction process.

(2) Girder height ratio. In view of the existing design practice and preliminary calculation assessment, the girder height in the span is consistent with that of the original bridge, which is 3.5 m. The girder height at the pivot point of the center pier is generally 1/16~1/20 of the calculated span diameter, and it is recommended that the girder height at the pivot point of the center pier be controlled between 1/15~1/28 of the main span diameter to ensure the stability and force performance of the bridge in actual use.

(3) Bottom plate thickness. The thickness of the bottom plate of box girder at the pivot point of the center pier is crucial in continuous Rigid-Frame Bridge because it determines the bearing capacity of the maximum compressive stress area, which directly affects the overall stability of the bridge and the control of deflection in the span. The thickness of the box girder bottom plate at the center pier fulcrum is selected to be 0.5~1.4m, and the thickness of the box girder bottom plate at the mid-span is set to be 1/4 of the thickness of the box girder bottom plate at the center pier fulcrum, and the reasonable thickness of the box girder bottom plate at the center pier fulcrum is determined by the positive stresses and deflections under the combination of the limit state loads in both the persistent condition and the transient condition. It is recommended that the thickness of the bottom plate at the center pier fulcrum should be set between 1/155 and 1/230 of the main span diameter to ensure the stability and reliability of the structure in long-term use.

IV. C. 2) Abutment Optimization

For the seismic performance of Rigid-Frame Bridge, this paper proposes to use ultra-high performance steel shell concrete (UHP-SSC) for the optimization of abutment.

(1) UHP-SSC box girder cross-section configuration

The UHP-SSC box girder height at the main span and the pier is 450cm and 1500cm respectively, the middle beam section is transitioned by 1.7 parabola, the length of the transverse unilateral cantilever section of the box girder is 110cm, the thickness of the box girder roof is 9cm, the thickness of the box girder bottom plate and the middle span of the box girder floor at the pier are 70cm and 9cm respectively, the thickness of the box girder web at the pier and the web thickness of the box girder in the span are 25cm and 14cm respectively, and the thickness of the inner and outer steel shells are 9mm. The roof and bottom plate are both stiffened to improve the local buckling capacity and facilitate the arrangement of prestressed steel bars, wherein the spacing, height and width of the roof and bottom plate stiffeners are 110cm, 15cm and 15cm respectively. The axillary dimensions of the peduncle of the top plate and the bottom plate of the box girder are 35cm×35cm and 18cm×18cm respectively, so as to reduce the influence of shear hysteresis effect and arrange the prestressed steel bar. The transverse force calculation shows that the spacing of the diaphragm is arranged according to 6.5m, and the UHPSSC plate with a thickness of 8.5cm is adopted, and the roof of the box girder can meet the requirements of structural strength and deformation.

(2) Construction program

The UHP-SSC box section is divided into several standard rod units and plate units, and the standard parts are all prefabricated in the factory, through high-temperature steam curing and adding micro-expansion agent to eliminate the early contraction of UHPC, avoiding the debonding and de-voiding between the UHPC and the steel shell, and ensuring the reliable transmission of force between the steel shell and the UHPC. The box girder is constructed by bridge crane or hanging basket at the construction site, which can not only hoist the whole section, but also hoist each basic component rod unit and plate unit on site, and assemble them into box girder sections at the bridge position, and the standard rod pieces and box girder sections are reliably connected by welding or high-strength bolts. In addition to the length of the main girder at the bridge abutment and the joint section, which is divided into 15m and 5m, the length of the other standard sections is 12m, and the weight of the corresponding sections ranges from 208.8t to 546.5t, and the lifting equipment of the sections adopts the bridge crane. During the construction process, the pre-arch is set to meet the linear requirement of the box girder design.

V. Conclusion

The article proposes a vibration characteristic analysis method of Rigid-Frame Bridge based on finite element software and modal analysis, and explores the optimization scheme of vibration damping design of Rigid-Frame Bridge through the simulation results of ground vibration.

(1) The difference between the first-tenth order frequency of Rigid-Frame Bridge obtained by using ANSYS software and the finite element model established by Simpack is no more than 0.46%, and the first-order transverse self-oscillating frequency of the whole bridge obtained by ANSYS software simulation is 0.581 Hz, which is higher than the standard specification (0.562 Hz). This shows that Rigid-Frame Bridge model established by using ANSYS finite element software can truly reflect its vibration, and the vibration pattern of the latter orders of Rigid-Frame Bridge is dominated by symmetrical bending in the middle span and side spans, and the overall intrinsic frequency is high and the stiffness is large.

(2) Under the action of seismic wave in the downstream direction, the displacement response in the downstream and transverse directions is small, except that the maximum and minimum values of the vertical displacement of Rigid-Frame Bridge are 1.39mm and -1.39mm, respectively. Under the action of seismic wave in the transverse direction, the maximum value of transverse displacement can reach 92.73mm, and the bridge overturning is more serious.

(3) For the seismic design of Rigid-Frame Bridge, this paper mainly optimizes the design from the two positions of main girder and abutment, and the main girder optimization mainly redesigns the side-to-span ratio, girder-height ratio and bottom plate thickness to achieve the purpose of seismic damping. While the abutment optimization is the introduction of ultra-high performance steel shell concrete optimization, and gives a specific construction plan, in order to better achieve the stable operation of Rigid-Frame Bridge.

References

[1] Elmy, M. H., & Nakamura, S. (2017). Static and seismic behaviours of innovative hybrid steel reinforced concrete bridge. Journal of Constructional Steel Research, 138, 701-713.

[2] Liu, C., & Gao, R. (2018). Design method for steel restrainer bars on railway bridges subjected to spatially varying earthquakes. Engineering structures, 159, 198-212.

[3] Saravanan, M., Goswami, R., & Palani, G. S. (2018). Replaceable fuses in earthquake resistant steel structures: A review. International Journal of Steel Structures, 18, 868-879.

[4] Qian, J., Zheng, Y., Dong, Y., Wu, H., Guo, H., & Zhang, J. (2022). Sustainability and resilience of steel–shape memory alloy reinforced concrete bridge under compound earthquakes and functional deterioration within entire life-cycle. Engineering Structures, 271, 114937.

[5] Kang, X., Jiang, L., Bai, Y., & Caprani, C. C. (2017). Seismic damage evaluation of high-speed railway bridge components under different intensities of earthquake excitations. Engineering Structures, 152, 116-128.

[6] Jiang, L., Kang, X., Li, C., & Shao, G. (2019). Earthquake response of continuous girder bridge for high-speed railway: A shaking table test study. Engineering Structures, 180, 249-263.

[7] Liu, C., Gao, R., & Guo, B. (2018). Seismic design method analyses of an innovative steel damping bearing for railway bridges. Engineering Structures, 167, 518-532.

[8] Xiang, N., & Li, J. (2020). Utilizing yielding steel dampers to mitigate transverse seismic irregularity of a multispan continuous bridge with unequal height piers. Engineering Structures, 205, 110056.

[9] Shen, X., Wang, X., Ye, Q., & Ye, A. (2017). Seismic performance of transverse steel damper seismic system for long span bridges. Engineering Structures, 141, 14-28.

[10] Akiyama, M., Frangopol, D. M., & Ishibashi, H. (2020). Toward life-cycle reliability-, risk-and resilience-based design and assessment of bridges and bridge networks under independent and interacting hazards: emphasis on earthquake, tsunami and corrosion. Structure and Infrastructure Engineering, 16(1), 26-50.

[11] Lin, Y., Zong, Z., Bi, K., Hao, H., Lin, J., & Chen, Y. (2020). Experimental and numerical studies of the seismic behavior of a steel-concrete composite rigid-frame bridge subjected to the surface rupture at a thrust fault. Engineering Structures, 205, 110105.

[12] Lai, Z., Kang, X., Jiang, L., Zhou, W., Feng, Y., Zhang, Y., ... & Nie, L. (2020). Earthquake influence on the rail irregularity on high‐speed railway bridge. Shock and Vibration, 2020(1), 4315304.

[13] Wang, B., Nishiyama, M., Zhu, S., Tani, M., & Jiang, H. (2021). Development of novel self-centering steel coupling beams without beam elongation for earthquake resilience. Engineering Structures, 232, 111827.

[14] Zhou, L., Wang, X., & Ye, A. (2019). Shake table test on transverse steel damper seismic system for long span cable-stayed bridges. Engineering Structures, 179, 106-119.

[15] Zeng, Q., & Dimitrakopoulos, E. G. (2018). Vehicle–bridge interaction analysis modeling derailment during earthquakes. Nonlinear Dynamics, 93, 2315-2337.

[16] Yılmaz, M. F., & Çağlayan, B. Ö. (2018). Seismic assessment of a multi-span steel railway bridge in Turkey based on nonlinear time history. Natural Hazards and Earth System Sciences, 18(1), 231-240.

[17] Hedayati Dezfuli, F., & Alam, M. S. (2017). Effect of different steel‐reinforced elastomeric isolators on the seismic fragility of a highway bridge. Structural Control and Health Monitoring, 24(2), e1866.

[18] Maleska, T., Nowacka, J., & Beben, D. (2019). Application of EPS geofoam to a soil–steel bridge to reduce seismic excitations. Geosciences, 9(10), 448.

[19] Mengyuan Xu,Qizhong Huang,Yang Yang,Hao Zhang,Zhe Sun & Yongjian Zheng. (2024). Theoretical and finite element methods for cross-section design of deep-sea flexible pipelines. Ocean Engineering(P3),119470-119470.

[20] Zhe Chen,Chao Ding,Zhen Liu & Shilin Sun. (2024). Finite element simulation analysis of vibration transmission characteristics of double shell based on ANSYS. Journal of Physics: Conference Series(1).
[21] Zhong Bao Ye,Rui Yuan Huang,Yong Chi Li,Lin Lv,Kai Zhao,Yong Liang Zhang... & Jia Jian Lin. (2018). Steel fiber-reinforced concrete under impact loading dynamic constitutive equation. Construction and Building Materials1049-1055.
[22] Qinglu Ma,Jianting Zhou,Saleem Ullah & Qi Wang. (2019). Operational modal analysis of rigid frame bridge with data from navigation satellite system measurements. Cluster Computing(3s),5535-5545.